Article

Study of Curing Characteristics of Cellulose Nanofiber-Filled Epoxy Nanocomposites

Mohan Turup Pandurangan * and Krishnan Kanny

Department of Mechanical Engineering, Durban University of Technology, Durban 4001, South Africa; kannyk@dut.ac.za
* Correspondence: mohanp@dut.ac.za; Tel.: +2-73-1373-2831

check for updates

Abstract: In recent years, much attention was focused on developing green materials and fillers for polymer composites. This work is about the development of such green nanofiller for reinforcement in epoxy polymer matrix. A cellulose nanofiber (CNF)-filled epoxy polymer nanocomposites was prepared in this work. The effect of CNF on curing, thermal, mechanical, and barrier properties of epoxy polymer is evaluated in this study. CNF were extracted from banana fiber using acid hydrolysis method and then filled in epoxy polymer at various concentration (0–5 wt.%) to form CNF-filled epoxy nanocomposites. The structure and morphology of the CNF-filled epoxy nanocomposites were examined by scanning electron microscopy (SEM) and transmission electron microscopy (TEM) analysis. Curing studies shows CNF particles acts as a catalytic curing agent with increased cross-link density. This catalytic effect of CNF particles has positively affected tensile, thermal (thermogravimetry analysis and dynamic mechanical analysis) and water barrier properties. Water uptake test of nanocomposites was studied to understand the barrier properties. Overall result also shows that the CNF can be a potential green nanofiller for thermoset epoxy polymer with promising applications ahead.

Keywords: thermoset polymer; epoxy; cellulose nanofiber; curing characteristics; thermal properties; mechanical properties

---

1. Introduction

Over the past two decades, much research attention focused on developing synthetic nanofillers such as carbon nanotubes (CNT), nanoclays, TiO_2, SiO_2, $CaCO_3$, and Al_2O_3, etc., for polymeric matrices. These nanofillers were reinforced in a range of polymeric matrices such as thermosets, thermoplastics, elastomers and their blends to develop polymer nanocomposites with nanofillers as reinforcement material. Dramatic improvements in thermal, mechanical, chemical, and physical properties were observed in nanoparticle filled in polymeric matrix composites [1–5]. However, in recent years because of the environmental pollution, rapid depletion in natural resources, recycling, and greenhouse carbon gas emission effects, researchers started looking for alternative green nanofillers for polymeric materials [6–8].

Some of the green nanofillers such as eggshell-based nanoparticles [9,10], plant-based materials [11–14] such as nanocellulose, lignin and hemicellulose, polylactic acid (PLA) [15,16], chitin/chitosan [17–19], etc., were the focus in recent past. Considerable breakthrough had been obtained with comparable thermo-mechanical properties using these green nanofillers to that of synthetic nanofillers.

In particular, plant-based cellulosic particles have gained a significant interest in the research communities because of their abundant availability and cost effective processing methods. Cellulose is abundantly available worldwide from plant source. Their availability is higher than that of commonly

produced synthetic materials such as polyethylene, polypropylene, PET, glass fibers, and carbon fibers. One observation suggests that cellulose fibril has a comparable tensile property to that of plain carbon steel material. Cellulose is an important component in the plant source which induces structural properties such as strength, stiffness, thermal, and physical stability. In general, cellulose content varies from 20 wt.% to 90 wt.% in plant source depending on the type of the plant [20–25].

Plants have three major chemical constituents, namely, cellulose, hemicellulose, lignin and other chemicals at minor level. Successful attempts have been made in the recent past regarding extraction of cellulosic material from plant source by chemical and physical methods [26–28]. Cellulose is available in the form of microfibril, nanocrystal, or nanofibers depending upon the obtainable size and processing methods [29,30].

These cellulosic particles were filled in polymer matrix to develop micro or nanocomposites, depending upon the size of the cellulosic particle fillers. In general, most of the literature focused on the addition of cellulosic particles in thermoplastic polymeric matrices, such as PP (polypropylene), LDPE (low density polyethylene), PLA (Polylactic acid), etc., [31–34]. The literature on cellulosic particles filled in thermoset polymers are relatively scarce or negligibly available [35]. It is important to understand the effect of these green nanoparticles on thermoset polymers such as epoxy, polyester, and urethanes. Thermoset epoxy and epoxy composites are widely used from bicycle industry to aerospace industry, because of their high thermal, mechanical, and barrier properties than that of polymeric materials [36,37]. A possible replacement of synthetic fillers with cellulosic nanofiber (CNF) fillers in thermosets will have huge impact on economic and social benefits.

Therefore, understanding the effect of CNF on thermal, mechanical, and barrier properties of the epoxy polymer matrix is vital as the study has significant industrial application. This paper focuses on the effect of CNF in epoxy polymer matrix on curing characteristics, structure, thermal, and mechanical properties. The sub-micron sized CNF were extracted from the stem section of banana fibers using acid hydrolysis method and the fibers were reinforced in the epoxy polymer to form epoxy-CNF nanocomposites.

2. Results and Discussion

Figure 1a shows the photograph image of raw banana fiber and CNF extracted from banana fiber. The raw banana fibers appear as a brown colored long fiber extracted from stem section of the banana plant. The CNF appears as a bright white colored particle, with above 95% cellulose content as obtained from our earlier study, with the CNF yield of ~28% from initial banana fiber mass content [38]. Figure 1b shows SEM image of cellulose nanofibers (CNF). The diameter of CNF varies from 50 nm to 100 nm and length 100 nm to 1000 nm. Figure 2 shows the TEM image of 2 wt.% CNF-filled epoxy nanocomposite (Figure 2a) and 5 wt.% CNF-filled epoxy nanocomposite (Figure 2b) observed under bright field mode. In this mode the CNF phase is represented by dark discontinuous needle like phase and the matrix phase is represented by bright continuous phase. Dispersion of CNF particles on the matrix was uniform at lower (2 wt.%) and higher concentration (5 wt.%). However, CNF particles tend to form agglomeration at higher concentration (5 wt.%).
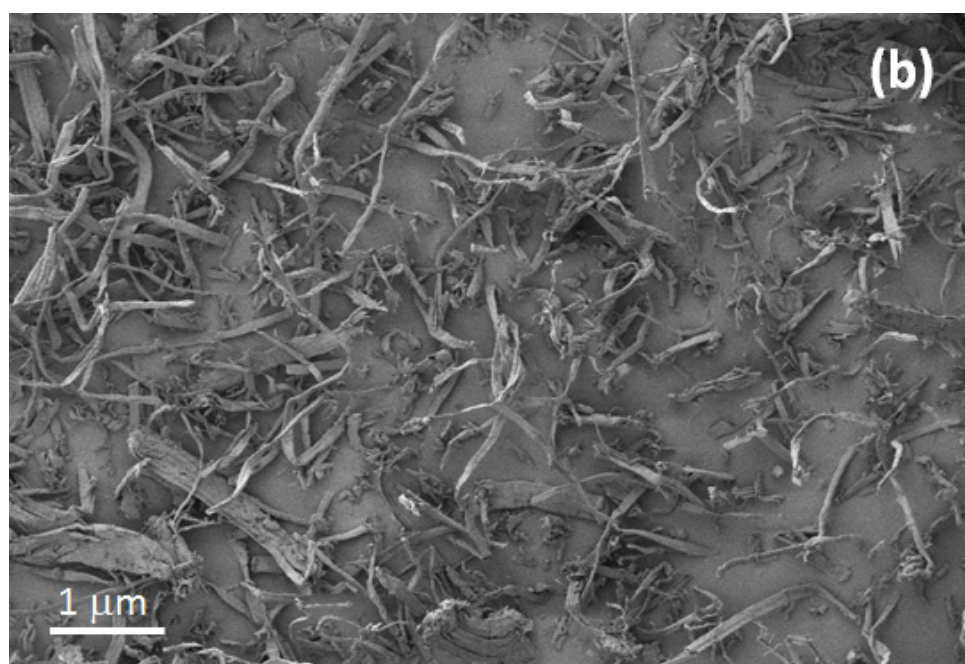
Figure 1. Fiber and cellulose nanofiber (CNF) images shows (**a**) photography image of raw banana fiber and extracted CNF; (**b**) SEM image of CNF fibrils.
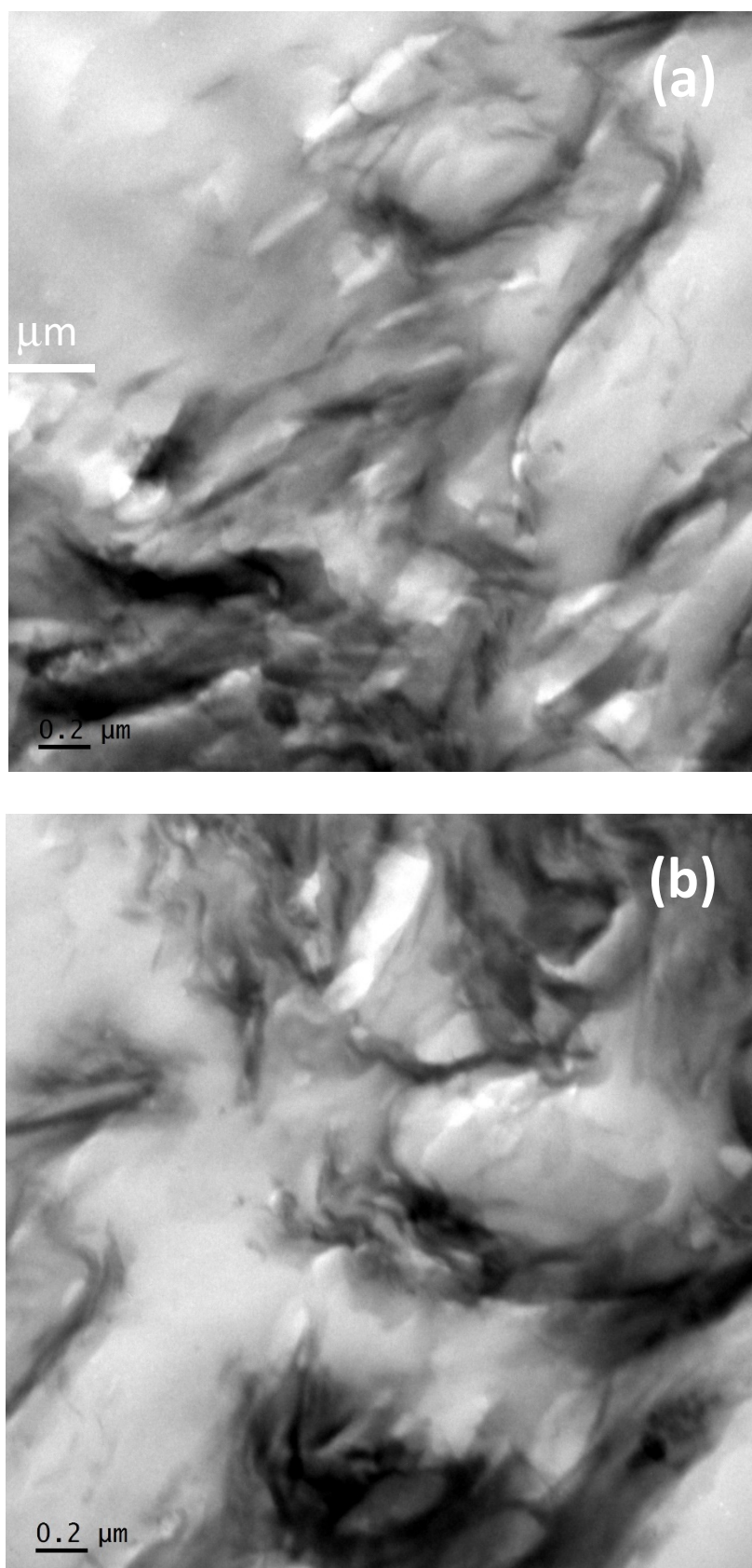
Figure 2. TEM image of epoxy with (**a**) 2 wt.% CNF; (**b**) 5 wt.% CNF-filled nanocomposites.

Figure 3 shows the measurement of heat release during gelation of epoxy and epoxy-CNF series during gelation. Unfilled neat epoxy resin shows the maximum heat release of 76 °C at around 96 min of gelation, whereas, epoxy with CNF up to 1 wt.% shows maximum heat release at relatively lower time around 90 min. The reduction in gelation time suggest the catalytic effect of CNF particles during epoxy curing. CNF with above 1 wt.% shows the gelation peak similar to that of neat epoxy resin, however, with reduced peak width as function of CNF concentration. This suggests the higher concentration may not act as a catalytic agent, however, it may aid faster curing. This curing characteristics of the of nanocomposite series was further examined using the FTIR study. Figure 4 shows the FTIR spectrum of CNF, unfilled neat cured epoxy polymer, 0.5 wt.% and 3 wt.% CNF-filled epoxy nanocomposites. CNF shows a broad band around 3400 cm^{-1} suggesting presence of –OH group. Presence of a shoulder at around 1660 cm^{-1} suggests oxidation of carbohydrate during CNF extraction. A peak around 1102 cm^{-1} is due to C–H stretching of the cellulosic group. A peak at 1102 cm^{-1} suggest changes induced in hydrogen bonds indicating transition from cellulose I to cellulose II structure during chemical treatment. A band at around 1034 cm^{-1} suggests a fraction of xyloglucans associated with non-hydrolyzed hemicellulose which is strongly bound within cellulosic fibrils. A sharp peak at around 888 cm^{-1} suggests a typical cellulosic structure [39,40]. Unfilled neat epoxy polymer shows a characteristics peak of a typical epoxy group (3500 cm^{-1} OH stretching vibration; shoulder at 2950 cm^{-1}–2775 cm^{-1} of CH stretching of CH_2 and CH aromatic or aliphatic vibration; 1608 cm^{-1} of aromatic C=C stretching; 1504 cm^{-1} of C-C stretching; 1031 cm^{-1} C–O–C of ether stretching; 830 cm^{-1} of oxirane group) [41,42]. The nanocomposites show almost all characteristics peaks of epoxy and CNF and suggest the presence of both these phases. However, in nanocomposites the intensity of oxirane peak (830 cm^{-1}) was reduced with the disappearance of carbohydrate oxidation peak of CNF (1660 cm^{-1}) in 0.5 wt.% CNF and 3 wt.% CNF-filled epoxy nanocomposites. This suggests that CNF might induce a catalytic curing of oxirane rings of epoxy polymer. The reduced oxirane peak shows the higher level of cross-link density of the epoxy polymer in nanocomposites due to CNF particles, possibly the oxidized cellulose in presence of amine curing agent induced amide bonding. This "amidated" cellulose molecules might have incorporated covalent bonding with epoxide structure, showing the presence of amide group's band at around 1660 cm^{-1} in nanocomposites. This effect suggests catalytic effect of CNF in epoxy polymer and may also affect the properties of composite.
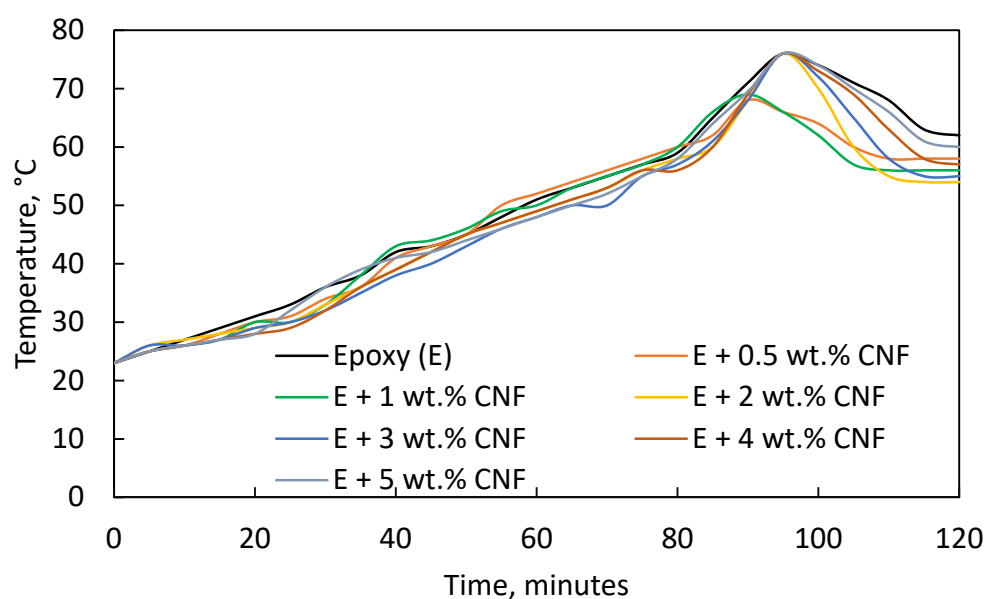

Figure 3. Time–temperature gelation of unfilled and CNF-filled epoxy nanocomposite series.
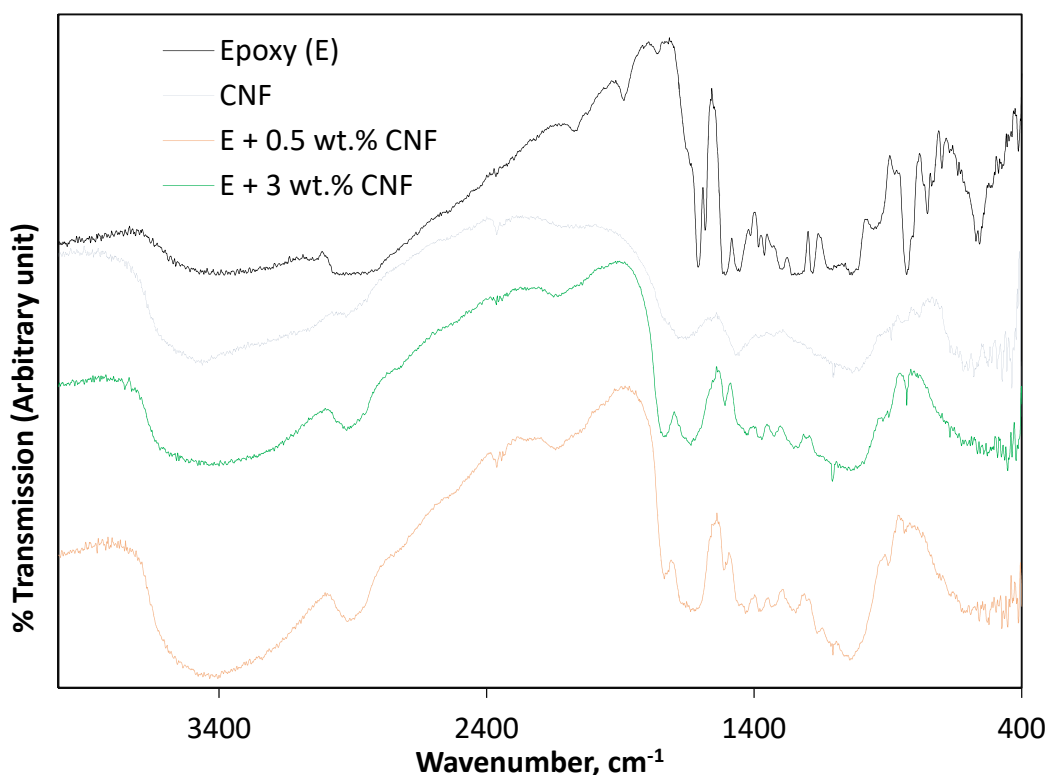
Figure 4. FTIR spectrum of CNF, epoxy and epoxy filled with 0.5 wt.% CNF and 3 wt.% CNF-filled nanocomposites.

Tensile properties of nanocomposites were examined and the tensile stress–strain curves are shown in Figure 5 with their values in Table 1. In general, tensile properties are positively affected because of the addition of CNF particles. Maximum improvement of 86% increased modulus at 5 wt.% CNF, 11% increased strength at 5 wt.% CNF, and an 26% increased elongation at 3 wt.% CNF was obtained than that of unfilled neat epoxy polymer. Although the general trend shows increased tensile properties of nanocomposites, Table 1 shows the tensile values are fluctuating as the function of CNF content. This could be due to the few factors, namely, inconsistent particle size, cellulose concentration within and among the particles, and other non-cellulosic phases presenting in the particles. Since the material was extracted from natural source such level inconsistence properties are expected. Similar results were also obtained elsewhere [8,31,33].

TGA of nanocomposites were examined and their plot is shown in Figure 6 with their values in Table 2. The thermal decomposition of CNF was lower than that of neat banana fiber. This could be due to the larger heat energy exposed by CNF due to its high surface area when compared with banana fiber [43]. Whereas, the thermal stability of the nanocomposite is higher than that of neat epoxy polymer, possible that the nanolevel dispersion of CNF particles acted as a thermal barrier to the epoxy polymer matrix and resulted in improved thermal stability. Similar improved thermal properties were also obtained in CNF-filled thermoplastic polymer nanocomposites [32,44]. Relatively lesser improvement at thermal property at higher content CNF (>3 wt.%) could be due to the higher amount of surface area exposure of particles. Much of the improvement in thermal stability is obtained at 2 to 3 wt.% CNF-filled epoxy nanocomposites.
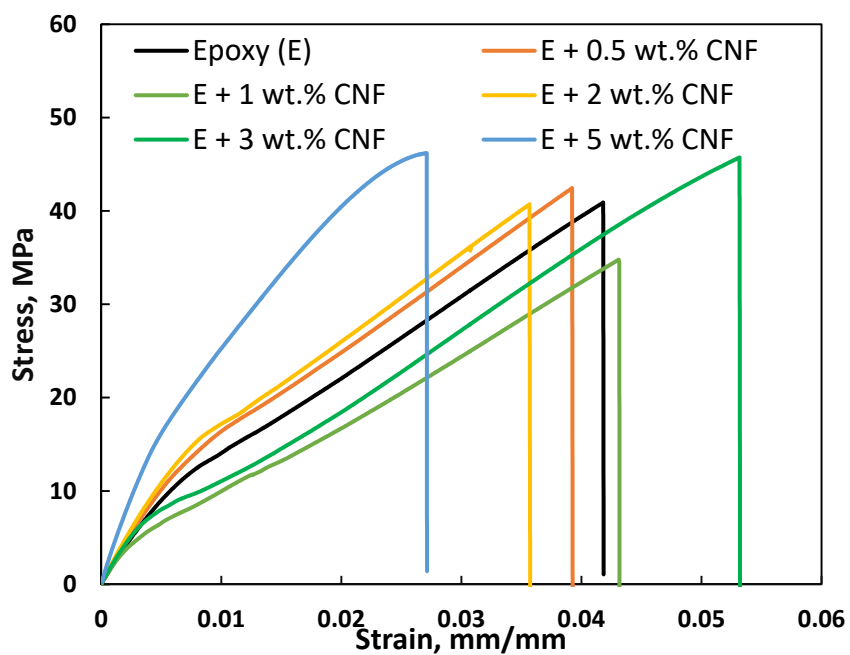
Figure 5. Tensile stress–strain curves of unfilled and CNF-filled epoxy nanocomposite series.

Table 1. Tensile properties of unfilled epoxy and CNF-filled epoxy nanocomposites.

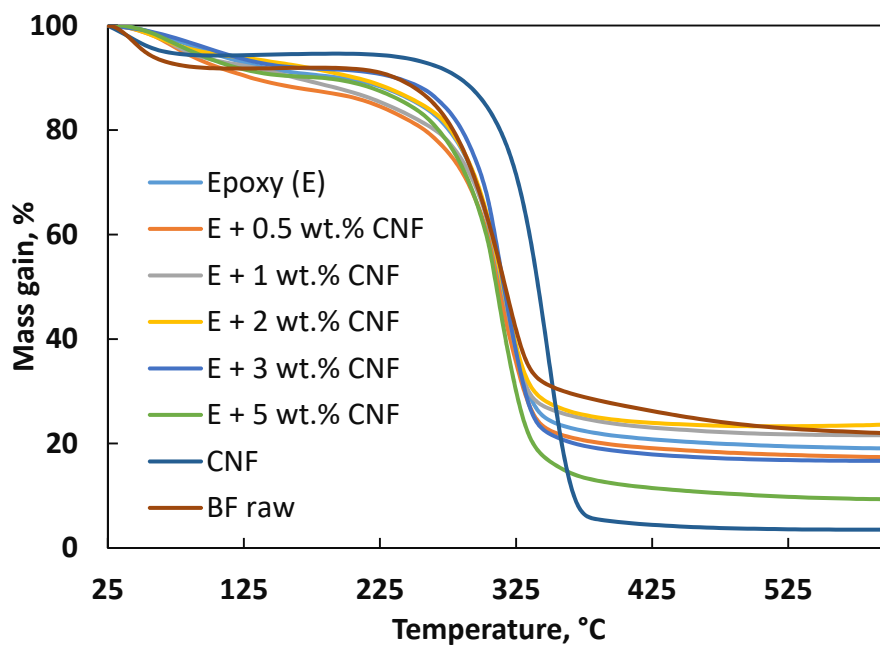| Material	Modulus, GPa	Ultimate Tensile Strength, MPa	Elongation at Break, %
Epoxy (E)	2.2	41.6	4.2
E + 0.5 wt.% CNF	2.2	42.3	3.9
E + 1 wt.% CNF	2.0	34.4	4.3
E + 2 wt.% CNF	2.4	40.6	3.5
E + 3 wt.% CNF	2.1	45.6	5.3
E + 5 wt.% CNF	4.1	46.2	2.7

Figure 6. TGA curves of unfilled and CNF-filled epoxy nanocomposite series.

Table 2. TGA properties of unfilled epoxy and CNF-filled epoxy nanocomposites.

Material	Mass Loss at 125 °C, %	Mass Loss at 200 °C, %	Mass Gain at 425 °C, %	Mass Gain at 525 °C, %	Onset Decomposition Temperature, °C	Mass Loss at Onset Decomposition, %	Endset Decomposition Temperature, °C	Mass Gain at Endset Decomposition, %
CNF	5.7	5.4	4.4	3.6	295	12.7	380	5.8
Banana fiber	8.2	8.2	26.2	22.9	255	12.8	350	31.7
Epoxy (E)	7.1	10.1	20.8	19.5	260	16.1	345	25.2
E + 0.5 wt.% CNF	9.5	13.5	19.1	17.8	270	22.8	345	23.3
E + 1 wt.% CNF	7.7	12.4	23.0	21.8	275	22.2	340	28.1
E + 2 wt.% CNF	6.2	9.6	24.0	23.3	265	16.7	340	29.5
E + 3 wt.% CNF	6.4	8.5	17.9	16.8	270	14.8	345	22.7
E + 5 wt.% CNF	8.4	10.6	11.5	9.8	265	19.1	350	16.6

Figure 7 shows the DMA properties of CNF-filled epoxy nanocomposite series with their properties in Table 3. The CNF addition increases the storage modulus of epoxy at room and elevated temperatures (Figure 7a). This improvement could be due to the hard and stiff properties of the CNF particles when compared with epoxy polymer matrix. Figure 7b shows the Tanδ versus temperature values of nanocomposite series. The temperature at which maximum Tanδ value obtained is called glass transition temperature (T_g). T_g is a temperature at which molecular relaxation occurs in the amorphous phase of the polymer and changes toward rubbery phase. Marginal increase in T_g value is obtained in nanocomposites due to the addition of CNF particles. The CNF particles possibly resisted the molecular relaxation movement during heating and increased the T_g temperature. The Tan δ peak value was reduced in composites (>1 wt.% CNF) than that of neat epoxy polymer. Similar results on the reduced Tan δ peak values were observed elsewhere, suggesting effective reinforcement of particles in the polymer matrix [35,45,46]. Tan δ peak value relates to damping and impact characteristics of the material. The reduction in Tan δ peak value in composites (>1 wt.% CNF) shows improved damping/impact characteristics due to increased packing efficiency of the CNF particles in the matrix [45,46]. DMA results show optimized improvement was observed at 2–3 wt.% nanocomposite.
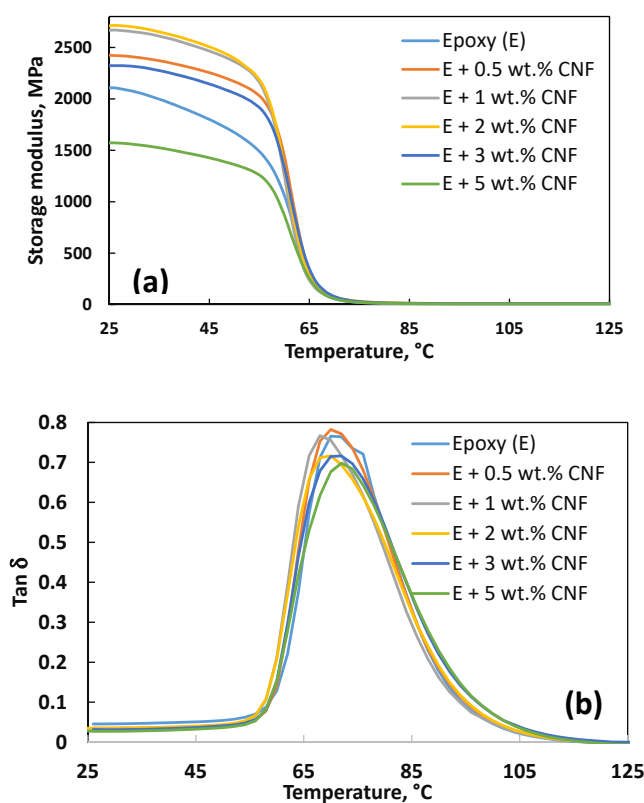

Figure 7. Dynamic mechanical analysis (DMA) of (**a**) storage modulus; (**b**) Tan δ of unfilled and CNF-filled nanocomposite series.

Table 3. DMA properties of unfilled epoxy and CNF-filled epoxy nanocomposites.

Material	Storage Modulus at 25 °C, MPa	Storage Modulus at 80 °C, MPa	Storage Modulus at 100 °C, MPa	T_g, °C	Tan δ Peak
Epoxy	2107	11.84	7.31	70	0.765
E + 0.5 wt.% CNF	2424	14.51	8.91	70	0.782
E + 1 wt.% CNF	2656	15.27	9.97	68	0.766
E + 2 wt.% CNF	2708	18.51	10.85	70	0.717
E + 3 wt.% CNF	2323	16.56	9.47	72	0.716
E + 5 wt.% CNF	1570	12.24	6.36	72	0.698

Water uptake properties of nanocomposites is shown in Figure 8 with their values in Table 4. When compared with neat epoxy polymer, water uptake is reduced in CNF-filled epoxy nanocomposites. The reduction in water uptake is proportional to CNF content in epoxy polymer matrix. Maximum reduction of ~47% decreased water uptake was observed in 5 wt.% CNF-filled epoxy nanocomposite than that of neat epoxy polymer. This reduction may be due to the hydrophobic characteristics of CNF particles than that of banana fiber [26–30] and possibly this effect would have resulted in improved water barrier properties of nanocomposites. Moreover, large surface of CNF particles might have exposed a larger area of water medium and served as a barrier medium and protected the matrix polymer against water uptake.
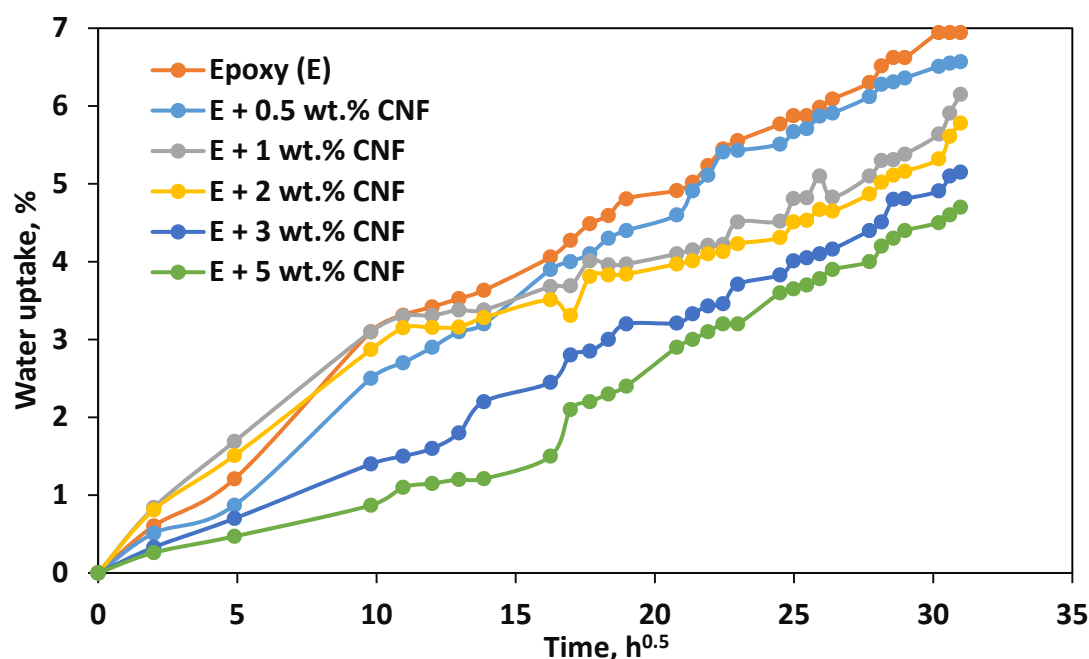
Figure 8. Water uptake of unfilled and CNF-filled epoxy nanocomposite series.

Table 4. Water uptake properties of unfilled epoxy and CNF-filled epoxy nanocomposites.

Material	Equilibrium Water Uptake, %
Epoxy (E)	6.94
E + 0.5 wt.% CNF	6.57
E + 1 wt.% CNF	6.15
E + 2 wt.% CNF	5.78
E + 3 wt.% CNF	5.15
E + 5 wt.% CNF	4.10

3. Materials and Methods

3.1. Raw Materials

The matrix material is a cured thermoset epoxy polymer made up of resin and hardener.

Epoxy resin (Diglycidyl ether of bisphenol-A) and hardener (unmodified cyclic aliphatic amine) supplied under trade name LR-20 and LH-281 respectively were obtained from AMT Composites (Mumbai, South Africa). Banana fibers were obtained from Richmond traders, Mumbai, India. The fibers were mechanically extracted from the stem part of the banana plant. All other chemicals used for the extraction of cellulose nanofibers were obtained from Merck Chemicals, Durban, South Africa.

3.2. Extraction of Cellulose Nanofiber (CNF)

CNF were extracted from banana fibers using acid hydrolysis process. Initially the banana fibers were cut into lengths of 3 cm. CNF extraction process involved three steps, namely, alkaline treatment, bleaching, and acid hydrolysis.

In alkaline treatment, the chopped banana fibers were soaked in 5 wt.% NaOH solution at the weight ratio of 1:10 of fiber to solution content. The fibers were soaked for 24 h after which the fibers were extracted and dried in an oven at 60 °C for 4 h.

In the bleaching process, alkaline-treated fibers were soaked and rinsed in concentrated sodium hypochlorite solution for 1 h. 3 wt.% fraction of fibers were soaked in a solution and bleached in running tap water. The fibers were removed and then placed in an oven at 60 °C for 4 h.

In the acid hydrolysis process, 10% of diluted sulfuric acid was prepared using distilled water in a beaker. Thereafter, bleached fibers were then soaked into the acid solution at 7 wt.% fiber weight fraction. The fiber-solution was stirred using a mechanical stirrer for 30 min. Thereafter, the excess liquid solution was extracted by a vacuum process. The acid-hydrolyzed fibers were then washed with distilled water and dried in an oven at 60 °C for 4 h.

In the above processes, cellulosic phase in the banana fiber was extracted and all other non-cellulosic phases such as lignin, hemicellulose, and other non-cellulosic phases were eliminated.

3.3. Processing of CNF-Filled Epoxy Nanocomposites

Synthesis of nanocomposites were carried out in two steps. First step involved mixing of resin with desired concentration of CNF and the second step involved casting of resin-hardener-CNF mixture in a glass mold. An electric shear mixer (Heidolph MR Hei: Standard, Labotec, South Africa) was used to mix resin and CNF particles. Initially, 100 g epoxy resin was heated in a glass beaker at 80 °C and CNF were added followed by shear mixing at 500 rpm for 0.5 h at 80 °C. The resin and CNF particle mixture were then cooled to room temperature (RT) and 30% weight fraction of hardener to that of epoxy resin (as per supplier's manual) was added into the mixture for curing purpose. The resin, hardener, and CNF together were gently stirred using a glass rod for ~3 min and then cast into glass molds. The casting process involved pouring of resin-hardener-CNF mixture in between two glass mold plates (30 cm × 30 cm × 3 cm) separated by a rubber gasket running along the three sides of the plates. The pouring of the resin mixture was assisted by a runner attached to the top side of the glass plate molds. To facilitate easier removal of the cast product, wax was used as a mold release agent and applied at the inner face of the glass plates and rubber gasket before the pouring process. The nanocomposite cast sample (with dimension of ~27 cm × 27 cm × 3 mm) was obtained 24 h after it was poured inside the mold cavity. The testing and characterization was carried out after seven days of curing (i.e., fully cured state of the epoxy polymer under experimental condition, though 100% curing cannot be achieved). The cured sheets were further cut and sized as per the standard dimension required for conducting testing.

3.4. Characterisation

A scanning electron microscope (SEM) was used to analyze the surface morphology of CNF particles. CNF surfaces were examined by Zeiss Environmental SEM (ESEM: model EVO HD 15 operating at controlled pressure conditions at 20 kV). Before conducting the actual SEM surface analysis, CNF specimens were gold surface-coated using Quorum-150R ES model thin film coating equipment.

A high-resolution transmission electron microscope (TEM) was used to study the dispersion of CNF particles in the epoxy polymer matrix. TEM was carried out on an ultrathin microtomed nanocomposite specimen using JEOL HR-TEM (JEM-2100 series), operating at 120 kV.

Thermogravimetric analysis (TGA) and dynamic mechanical analysis (DMA) were used to examine the thermal properties of nanocomposites using TA instruments SDT Q600 model and Q800 model respectively. In TGA, thermal properties of nanocomposites such as weight loss, decomposition temperature, and degradation were evaluated. In TGA analysis, ~5 mg of the sample was placed in an alumina crucible of TA apparatus and the sample was scanned from RT to 600 °C at a scanning rate of 10 °C/min under atmospheric condition.

DMA testing on nanocomposites was carried out at a frequency of 10 Hz using a 3-point bending mode of TA instrument from 25 °C to 125 °C under atmospheric conditions. In DMA testing, specimen dimension of 5.5 cm × 1 cm × 0.3 cm was used. DMA parameters such as storage modulus, Tanδ (damping factor) and T_g (glass transition temperature) were measured using DMA.

FTIR (Nicolet) analysis was carried out for the cured epoxy and epoxy-CNF nanocomposite series using an attenuated total reflectance (ATR) mode to study the functional group of epoxy and curing characteristics of nanocomposites. Moreover, curing characteristics of epoxy and epoxy-CNF nanocomposite were studied by directly monitoring the exothermic cure temperature at regular time intervals. The temperature of the curing reaction was recorded at regular intervals as soon as the hardener was mixed into the epoxy resin. The time–temperature graph was plotted for all the curing sample series.

3.5. Testing

The tensile test of nanocomposite series was conducted on the cured samples to study the tensile modulus, strength, and elongation properties of CNF-filled epoxy composites. The tensile test was conducted as per ASTM D3039 standard test, with specimen dimension of 5 cm gauge length × 1 cm width × 0.3 cm thick. The tensile test was conducted using an MTS UTM Tensile Tester (Model LPS 304—424708 series) with a crosshead speed of 1 mm/min and 1kN load cell. A mean value of tensile property of three specimens was selected and considered for analysis.

Barrier properties of nanocomposites was studied by a water immersion test method, as per ASTM D570-98 (2005) test procedure at 25 °C. Three test specimens, each of dimension 3 cm × 3 cm × 0.3 cm, were chosen for this study. In order to eliminate surface or subsurface entrapped moisture and retain actual solid mass in the specimen, test samples were dried at 60 °C for 4 h using an oven. During the 4 h drying, samples were taken out of the oven at an interval of 1 h and immediately transferred into the airtight desiccator. The RT-cooled sample was weighed and ensured that the mass loss remained constant until the 4 h heating cycle.

The actual solid mass sample was then immediately taken out of the desiccator and fully immersed in a distilled water medium which was placed in a temperature-controlled water bath set-up. The bath temperature was constantly maintained at 25 °C for entire duration of the water immersion test. The water soaked specimen was taken from the water bath at different time intervals and wiped using a paper towel to eliminate surface water. The sample was then weighed in an electronic balance and then immediately transferred back into the water bath set-up. This weighing procedure was repeated until

the water soaked sample showed no or negligible increase in the water mass uptake (i.e., equilibrium water uptake content, W_e). The W_e was measured as per Equation (1)

$$W_e = \frac{(W_t - W_i)}{(W_i)} \times 100 \tag{1}$$

where W_i and W_t are initial dry solid mass of the test specimen and the water mass uptake of soaked sample at time t of testing was done respectively. The barrier property was examined by selecting the mean test specimen water uptake result.

4. Conclusions

In this work, polymer nanocomposites consisting of CNF particles as reinforcement filler and thermoset epoxy polymer were produced by shear mixing process. The prime objective of this study is to prepare a CNF-filled thermoset polymer-based composites. CNF particles were filled up to 5 wt.% in epoxy polymer matrix. The effect of CNF concentration on curing tensile, DMA, TGA, and water uptake properties was evaluated. CNF addition shows positive effect in these properties. FTIR and curing studies shows that CNF may act as a curing catalyst during epoxy gelation and increases the cross-link density of the epoxy polymer and reduces with curing time. Well-dispersed CNF particles were obtained in this processing method. Almost comparable modulus, 10% increased tensile strength and 26% increased elongation were observed in 3 wt.% CNF-filled epoxy nanocomposite. An optimized improved onset and endset decomposition temperature was observed at 2–3 wt.% CNF-filled epoxy nanocomposite. In the DMA study, storage modulus of 2 wt.% CNF-filled epoxy nanocomposite was increased by 28%, 56%, and 48% respectively at 25 °C, 80 °C, and 100 °C respectively when compared with unfilled epoxy polymer. Water uptake results suggest that the water uptake proportionally reduces in nanocomposites as concentration of CNF particles increases in matrix polymer. Maximum 47% reduction of water mass uptake was seen in 5 wt.% CNF-filled epoxy nanocomposite. Overall results suggest that an optimum level of improvement is obtained at 2–3 wt.% CNF-filled epoxy nanocomposite. The result suggests that the CNF can be successfully incorporated in thermoset epoxy polymer matrix with improved properties and serve as a promising green nanofiller for the epoxy matrix.

Author Contributions: M.T.P. conducted the study, analyzed the result and wrote the paper. K.K. was project supervision and fact checking of scientific claims in the manuscript. Both the authors together formulated the objective of the manuscript. All authors have read and agreed to the published version of the manuscript.

Conflicts of Interest: The authors declare no conflict of interest.

References

1. Valentino, O.; Melanie, M.; George, P.S.; Landi, G.; Neitzert, H.-C. The effect of the nanotube oxidation on the rheological and electrical properties of CNT/HDPE nanocomposites. *Polym. Eng. Sci.* **2017**, *57*, 665–673.
2. Fei, H.; Wenjian, Z.; Armin, T.R.; Nieh, M.P.; Cornelius, C.J. SiO$_2$-TiO$_2$-PBC nanocomposite film morphology, solvent swelling, estimated parameter, and liquid transport. *Polymer* **2017**, *123*, 247–257.
3. He, H.; Li, K.; Wang, J.; Sun, G.; Li, Y.; Wang, J. Study on thermal and mechanical properties of nano-calcium carbonate/epoxy composites. *Mater. Des.* **2011**, *32*, 4521–4527. [CrossRef]
4. Yang, Q.; Lin, Y.; Li, M.; Shen, Y.; Nan, C.-W. Characterization of mesoporous silica nanoparticle composites at low filler content. *J. Compos. Mater.* **2016**, *50*, 715–722. [CrossRef]
5. Velmurugan, R.; Mohan, T.P. Epoxy–Clay Nanocomposites and Hybrids: Synthesis and Characterization. *J. Reinf. Plast. Compos.* **2009**, *28*, 17–37. [CrossRef]
6. Xu, Q.; Wang, Y.; Chi, M.; Hu, W.; Zhang, N.; He, W. Porous polymer-titanium dioxide/copper composite with improved photocatalytic activity toward degradation of organic pollutants in wastewater: Fabrication and characterization as well as photocatalytic activity evaluation. *Catalysts* **2020**, *10*, 310. [CrossRef]

7. Giuseppina, L.; Claudio, I.; Giuseppe, V. Photosensitive hybrid nanostructured materials: The big challenges for sunlight capture. *Catalysts* **2020**, *10*, 103.

8. Kargarzadeh, H.; Huang, N.; Lin, I.; Ahmad, M.; Mariano, A.; Dufresne, A.; Thomas, S.; Galeski, A. Recent developments in nanocellulose-based biodgradable polymers, thermoplastic polymers, and porous nanocomposites. *Prog. Polym. Sci.* **2018**, *87*, 197–227. [CrossRef]

9. Punyanich, I.; Aroon, K.; Kavichat, K. The potential of chicken eggshell waste as a bio-filler filled epoxidized natural rubber (ENR) composite and its properties. *J. Polym. Environ.* **2013**, *21*, 245–258.

10. Munlika, B.; Kaewta, K. Biodegradation of thermoplastic starch/eggshell powder composites. *Carbohydr. Polym.* **2013**, *97*, 315–320.

11. Gallo, E.; Schartel, B.; Acierno, D.; Cimino, F.; Russo, P. Tailoring the flame retardant and mechanical performances of natural fibre-reinforced biopolymer by multi-component laminate. *Compos. B Eng.* **2013**, *44*, 112–119. [CrossRef]

12. Zuhri, M.Y.M.; Guan, Z.W.; Cantwell, W.J. The mechanical properties of natural fibre based honeycomb core materials. *Compos. B Eng.* **2014**, *58*, 1–9. [CrossRef]

13. Sanjay, M.R.; Suchart, S.; Jyotishkumar, P.; Jawaid, M.; Pruncu, C.I.; Khan, A. A comprehensive review of techniques for natural fibers as reinforcement in composites: Preparation, processing and characterization. *Carbohydr. Polym.* **2019**, *207*, 108–121.

14. Engin, S.; Hasan, C.; Hakan, D. Production of epoxy composites reinforced by different natural fibers and their mechanical properties. *Compos. B Eng.* **2019**, *167*, 461–466.

15. Mohamadreza, N.; Dilara, S.; Pierre, J.C.; Kamal, M.R.; Heuzey, M.-C. Poly (lactic acid) blends: Processing, properties and applications. *Int. J. Biol. Macromol.* **2019**, *125*, 307–360.

16. Jin, F.-L.; Hu, R.-R.; Park, S.J. Improvement of thermal behaviors of biodegradable poly (lactic acid) polymer: A review. *Compos. B Eng.* **2019**, *164*, 287–295. [CrossRef]

17. Nguyen, M.A.; Wyatt, H.; Susser, L.; Geoffrion, M.; Rasheed, A.; Duchez, A.-C.; Cottee, M.L.; Afolayan, E.; Farah, E.; Kahiel, Z.; et al. Delievery of microRNAs by chitosan nanoparticles to functionally alter macrophage cholesterol efflux in vitro and in vivo. *ACS Nano* **2019**, *13*, 6491–6505. [CrossRef]

18. Nooshin, V.; Farhad, G.; Behjat, T.; Cacciotti, I.; Jafari, S.M.; Omidi, T.; Zahedi, Z. Biodegradable zein film composites reinforced with chitosan nanoparticles and cinnamon essential oil: Physical, mechanical, structural and antimicrobial attributes. *Colloids. Surf. B* **2019**, *177*, 25–32.

19. Monika, Y.; Priynshi, G.; Kunwar, P.; Kumar, M.; Pareek, N.; Vivekanand, V. Seafood waste: A source for preparation of commercially employable chitin/chitosan materials. *Bioresour. Bioprocess.* **2019**, *6*, 8.

20. Mondher, H.; Abderrahim, E.M.; Zouhaier, J.; Akrout, A.; Haddar, M. Static and fatigue characterization of flax fiber reinforced thermoplastic composites by acoustic emission. *Appl. Acoust.* **2019**, *147*, 100–110.

21. Amy, L.; William, P.; Shannon, B.; Frantz, D.; Burholder, J.; Kiziltas, A.; Mielewski, D. Heat-treated blue agave fiber composites. *Compos. B Eng.* **2019**, *165*, 712–724.

22. Dang, C.-Y.; Shen, X.-J.; Nie, H.-J.; Yang, S.; Shen, J.-X.; Yang, X.-H.; Fu, S.-Y. Enchanced interlaminar shear strength of ramie fiber/polypropylene composites by optimal combination of graphene oxide size and content. *Compos. B Eng.* **2019**, *168*, 448–495. [CrossRef]

23. Abraham, E.; Thomas, M.S.; John, C.; Pothan, L.A.; Shoseyov, O.; Thomas, S.; Smith, R.H. Green nanocomposites of natural rubber/nanocellulose: Membrane transport, rheological and thermal degradation characterisations. *Ind. Crop. Prod.* **2013**, *51*, 415–424. [CrossRef]

24. Codispoti, R.; Oliveira, D.V.; Olivito, R.S.; Paulo, B.L.; Fangueiro, R. Mechanical performance of natural fiber-reinforced composites for the strengthening of masonry. *Compos. B Eng.* **2015**, *77*, 74–83. [CrossRef]

25. Mohan, T.P.; Kanny, K. Nanoclay infused banana fiber and its effects on mechanical and thermal properties of composites. *J. Compos. Mater.* **2016**, *50*, 261–276. [CrossRef]

26. Roni, M.d.S.; Wilson, P.F.N.; Hudson, A.S.; Dantas, N.O.; Neto, W.P.F. Cellulose nanocrystals from pineapple leaf, a new approach for thereuse of this agro-waste. *Ind. Crop. Prod.* **2013**, *50*, 707–714.

27. Ligia, M.M.C.; Gabriel, M.d.O.; Bibin, M.C.; Leao, A.L.; de Souza, S.F.; Ferreira, M. Bionanocomposites from electrospun PVA/pineapple nanofibers/Stryphnodendron adstringens bark extract for medical applications. *Ind. Crop. Prod.* **2013**, *41*, 198–202.

28. Li, J.; Wei, X.; Wang, Q.; Chen, J.; Chang, G.; Kong, L.; Su, L.; Liu, Y. Homogeneous isolation of nanocellulose from sugarcane bagasse by high pressure homogenization. *Carbohydr. Polym.* **2012**, *90*, 1609–1613. [CrossRef]

29. Erika, M.; Riccardo, R.; Marco, A.O.; Simone, G.B.; Luciano, P. Comparison of cellulose nanocrystals obtained by sulphuric acid hydrolysis and ammonium persulfate, to be used as coating on flexible food-packaging materials. *Cellulose* **2016**, *23*, 779–793.

30. Fleur, R.; Mohamed, N.B.; Alessandro, G.; Bras, J. Recent advances in surface-modified cellulose nanofibrils. *Prog. Polym. Sci.* **2019**, *88*, 241–264.

31. Maiju, H.; Kristiina, O. Pelletized cellulose fibres used in twin-screw extrusion for biocomposite manufacturing: Fibre breakage and dispersion. *Compos. Part A Appl. Sci. Manuf.* **2018**, *109*, 538–545.

32. Xu, K.; Liu, C.; Kang, K.; Zheng, Z.; Wang, S.; Tang, Z.; Yang, W. Isolation of nanocrystalline cellulose from rice straw and preparation of its biocomposites with chitosan: Physicochemical characterization and evaluation of interfacial compatibility. *Compos. Sci. Technol.* **2018**, *154*, 8–17. [CrossRef]

33. Goeun, S.; Yanqing, L.; van de Ven, T. Transparent composite films prepared from chemically modified cellulose fibers. *Cellulose* **2016**, *23*, 2011–2024.

34. Sinke, H.O.; Christina, D.; Sven, F.; Andres, B.; Engstrand, P.; Norgren, S.; Engström, A.-C. Nanofibrillated cellulose/nanographite composite films. *Cellulose* **2016**, *23*, 2487–2500.

35. Saba, N.; Ahmad, S.; Sanyang, M.L.; Andres, B. Thermal and dynamic mechanical properties of cellulose nanofibers reinforced epoxy composites. *Int. J. Biol. Macromol.* **2017**, *102*, 822–828. [CrossRef] [PubMed]

36. Ziaullah, K.; Yousif, B.F.; Mainul, I. Fracture behaviour of bamboo fiber reinforced epoxy composites. *Compos. B Eng.* **2017**, *116*, 186–199.

37. Zheng, N.; Huang, Y.; Liu, H.-Y.; Gao, J.; Mai, Y.W. Improvement of interlaminar fracture toughness in carbon fiber/epoxy composites with carbon nanotubes/polysulfone interleaves. *Compos. Sci. Technol.* **2017**, *140*, 8–15. [CrossRef]

38. Sifiso, P.N.; Krishnan, K. Extraction of hemicellulose and lignin from sugarcane bagasse for biopolymer films: Green process. *J. Adv. Mater. Process.* **2018**, *6*, 57–65.

39. Heloisa, T.; Franciele, M.P.; Florencia, C.M. Cellulose nanofibers produced from banana peel by chemical and enzymatic treatment. *LWT Food Sci. Technol.* **2014**, *59*, 1311–1318.

40. Alemdar, A.; Sain, M. Biocomposites from wheat straw nanofibers: Morphology, thermal and mechanical properties. *Compos. Sci. Technol.* **2008**, *68*, 557–565. [CrossRef]

41. Patterson, W.A. Infrared absorption bands characteristic of oxirane rings. *Anal. Chem.* **1954**, *26*, 823–835. [CrossRef]

42. Chike, K.E.; Myrick, M.L.; Lyon, R.E.; Angel, S.M. Raman and near infrared studies of an epoxy resin. *Appl. Spectrosc.* **1993**, *47*, 1631–1635. [CrossRef]

43. Ticiane, T.; Luana, A.S.; Simone, M.L.R.; Bica, C.I.D.; Nachtigall, S.M.B. Cellulose nanocrystals from acacia bark–Influence of solvent extraction. *Int. J. Biol. Macromol.* **2017**, *101*, 553–561.

44. Abeer, A.; Amira, E.; Atef, I.; El-Shafei, A.M.; Kamar, M. Extraction of oxidized nanocellulose from date palm (Phoenix Dactylifera, L.) sheath fibers: Influence of CI and CII polymorphs on the properties of chitosan/bionanocomposite films. *Ind. Crop. Prod.* **2018**, *124*, 155–165.

45. George, T.M.; Abraham, E.; Jyotishkumar, P.; Maria, H.J.; Pothen, L.A.; Thomas, S. Nanocelluloses from jute fibers and their nanocomposites with natural rubber: Preparation and characterization. *Int. J. Biol. Macromol.* **2015**, *81*, 768–777.

46. Joseph, S.; Sreekala, M.S.; Oommen, Z.; Koshy, P.; Thomas, S. A comparison of the mechanical properties of phenol formaldehyde composites reinforced with banana fibres and glass fibres. *Compos. Sci. Technol.* **2002**, *62*, 1857–1868. [CrossRef]